

# Deep cryogenic treatment of HPDC AZ91 magnesium alloys prior to aging and its influence on alloy microstructure and mechanical properties

Preciado [Mónica](#)  
mpreciado@ubu.es

Pedro Miguel [Bravo](#)  
pbravo@ubu.es

David [Cárdenas](#)  
dcardenas@ubu.es

University of Burgos, Department of Civil Engineering, Avda. Cantabria s/n, 09006 Burgos, Spain

\*Corresponding author.

---

## Abstract

Studies of deep cryogenic treatment have mainly focused on ferrous alloys, despite the advantages of this form of treatment when applied to other non-ferrous alloys. This study examines the microstructural behavior of a high pressure die-casting (HPDC) AZ91 magnesium alloy, submitted to T6 and T6 with deep cryogenic treatment (DCT) prior to aging. Differences between continuous and discontinuous  $\beta$ -Mg<sub>17</sub>Al<sub>12</sub> phase precipitation are analyzed by means of TEM, SEM and optical microscopy to explain the mechanical behavior following each type of heat treatment. The mechanical properties were improved by both treatments though yield strength was higher following T6 treatment and elongation was greater following T6 with deep cryogenic treatment. The conclusion is that continuous precipitation is promoted by cryogenic treatment, resulting in an improvement of elongation by 20%. This factor is important in view of the limitations of poor plasticity and its consequences for HPDC magnesium alloy applications.

---

**Keywords:** HPDC magnesium alloys; Deep cryogenic treatment; Continuous precipitation

## 1 Introduction

Magnesium alloys are generating greater interest as a manufacturing material in the automobile industry, due to their low density, high specific strength and weight reduction, as well as consequent savings on fuel consumption. Nevertheless, the use of magnesium alloys has been limited by the fact that due to their h.c.p. crystallization system, they must be formed plastically at temperatures exceeding 200 °C to activate the necessary number of slip systems, as stated by [Wetengen \(1993\)](#). Some studies have been conducted to improve weaknesses in the deformation behavior of these alloys through grain refining like [Mukai et al. \(2001\)](#) research, and [Luo and Pekguleryuz \(1994\)](#) made a review of the influence of alloying elements on cast magnesium alloys mechanical properties. AZ91D is one of the best commercial magnesium alloys, on account of its good combination of castability, mechanical strength, and ductility.

High Pressure Die Casting (HPDC) is the preferred manufacturing process for the magnesium alloy components used in automobiles, as well as in many other applications. The combination of HPDC and AZ91D, despite the above-mentioned properties, also presents a microstructure with a large quantity of pores. [Wang et al. \(2011\)](#) tried to quantify the gas content this type of castings and [Li et al. \(2015\)](#) studied the influence of this porosity during tensile deformation. Micropores form during the solidification of these alloys primarily due to dissolved gases and shrinkage.

All of the above is aggravated by the fact that high quantities of Al mean weaker ductility as fragile intermetallic (predominantly phase  $\beta$  or Mg<sub>17</sub>Al<sub>12</sub>) phases are formed in the grain boundaries. In general, a much more uniform microstructure could be achieved through solution treatments followed by controlled precipitation treatment. Nevertheless, while some authors like [Ji et al. \(2006\)](#) have pointed out that HPDC of magnesium alloys are not right for solution treatments, because of blister formation resulting from sub-surface pores, others like [Cavaliere and De Marco \(2007\)](#), have contended that it brings improvements in such properties as strength, elongation and fatigue after this type of treatment.

Furthermore, the application of low-temperature or Deep Cryogenic Treatment (DCT) has begun over recent decades, to improve the mechanical properties of the metals. Although this type of treatment has

mainly been applied to ferrous alloys like [Jordine \(1996\)](#) and [Preciado et al. \(2006\)](#), that studied the effect on carburized steels, its application to other types of alloys has also shown good results: [Chen et al. \(2001\)](#) and [Lulay et al. \(2002\)](#) studied the effects of cryogenic treatments on aluminum alloys and [Yuan et al. \(2015\)](#) on pure zirconium. There is increasing information on the effects of these treatments on the mechanical properties of magnesium alloys. For AZ91, [Asl et al. \(2009\)](#) observed an improvement in creep and wear behaviors and [Jiang et al. \(2010\)](#) obtained higher values of tensile strength and hardness after DCT in as-cast samples, [Amini et al. \(2014\)](#) found better hardness and wear resistance after DCT between solution and aging treatments and [Li et al. \(2013\)](#) obtained increased tensile strength and elongation with a multi-step treatment of solution and aging-DCT-aging.

DCT differs from Cold Treatments (CT) with regard to the temperatures to which the materials are subjected. Normally, the temperature for DCT is the boiling point of nitrogen at 77 K. This treatment may be done both before and after aging, knowing that the growth of the precipitates will be influenced by cryogenic temperatures. In this study, cryogenic treatment was done prior aging during a solution-aging treatment (T6).

## 2 Experimental procedure

The composition of the magnesium alloy AZ91D selected for this study was as follows (wt.%): Al, 8.83; Be, 0.001; Cu, 0.007; Fe, 0.003; Mn, 0.32; Si, 0.028 and Zn, 0.6. The samples were prepared for metallographic observation by milling and polishing to 1  $\mu\text{m}$ , following with acetic glycol etchant. The microstructure of the alloy after the HPDC process is shown in [Fig. 1](#) and consists of grains of Mg covered with precipitate at the grain edges, which corresponds to a divorced eutectic compound of  $\text{Mg-Mg}_{17}\text{Al}_{12}$ . Pores may also be appreciated that are situated on the grain boundaries.

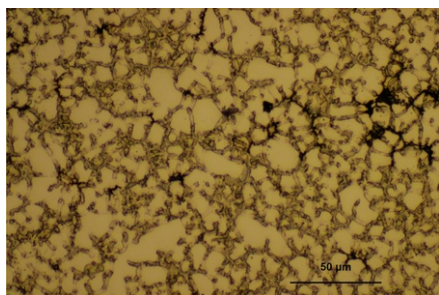


**Fig. 1** Microstructure of HPDC AZ91D. Grains of Mg with eutectic at the grain edges.

alt-text: Fig. 1

Specimens were fabricated for the tensile tests following the same process, so as to reproduce the porosities and the non-uniform microstructure of the real pieces. The shape was cylindrical, the gauge length was 30 mm, the diameter 5.9 mm and the velocity 10 mm/min. The specimens were injected in a mold, with the feeding in an extreme and the skin was not removed.

Tomographic images were taken of the specimens in the tests to assess whether the test zone was sufficiently free from porosities to obtain reliable results. The result ([Fig. 2](#)) was satisfactory in the sense that porosity in the test zone is less than  $48 \mu\text{m}^3$  and only the clamping heads had large-sized pores.

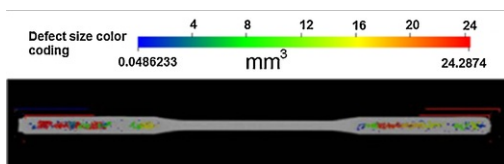


**Fig. 2** Tomography of the specimen for the tensile test.

alt-text: Fig. 2

These specimens were subjected to a T6 solution-aging test and to a combined T6-DCT prior to aging. The different treatments are summarized in [Table 1](#). The two-stage artificial aging was claimed to be an optimal treatment for the type of manufactured pieces by the company that supplied the test samples. The deep cryogenic treatment was only applied to samples that had been solubilized for 4 and 8 h, as the 18-h solution presented no appreciable improvement in mechanical properties. The cryogenic treatment consisted of a slow cool-down ( $\approx 1 \text{ }^\circ\text{C}/\text{min}$ ) from ambient temperature to liquid nitrogen temperature. When the

materials reached approximately  $-190\text{ }^{\circ}\text{C}$ , were held at that temperature for 22 h. Finally, the samples were allowed to warm up to room temperature. The time between the end of the deep cryogenic treatment and the aging was approximately of 4 h.

**Table 1** Thermal treatments applied to the different samples.

alt-text: Table 1

Route A	Solution ( $413\text{ }^{\circ}\text{C}$ for 4 h) + Aging ( $205\text{ }^{\circ}\text{C}$ for 4 h + $260\text{ }^{\circ}\text{C}$ for 1 h)
Route B	Solution ( $413\text{ }^{\circ}\text{C}$ for 8 h) + Aging ( $205\text{ }^{\circ}\text{C}$ for 4 h + $260\text{ }^{\circ}\text{C}$ for 1 h)
Route C	Solution ( $413\text{ }^{\circ}\text{C}$ for 18 h) + Aging ( $205\text{ }^{\circ}\text{C}$ for 4 h + $260\text{ }^{\circ}\text{C}$ for 1 h)
Route D	Solution ( $413\text{ }^{\circ}\text{C}$ for 4 h) + Deep Cryogenic Treatment + Aging ( $205\text{ }^{\circ}\text{C}$ for 4 h + $260\text{ }^{\circ}\text{C}$ for 1 h)
Route E	Solution ( $413\text{ }^{\circ}\text{C}$ for 8 h) + Deep Cryogenic Treatment + Aging ( $205\text{ }^{\circ}\text{C}$ for 4 h + $260\text{ }^{\circ}\text{C}$ for 1 h)
Route F	No treatment

A comparative study was performed of the different routes by means of ductility tests. Four samples were employed for each route except for route F with only two samples.

The samples were studied by TEM in a JEOL JEM 2100 microscope by carbon replica technique. The differences in precipitation were observed both in samples subjected to the T6 treatment and in samples with the deep cryogenic treatment (T6 + DCT).

### 3 Results

A set of tensile tests were conducted for a comparative study of the different routes. Four samples were used for each route, except for route F that only had two samples.

Tensile testing results are summarized in [Fig. 3](#) and [Table 2](#). The values and curves correspond to the mean values. In the true stress-strain graph, strain hardening for different heat treatments may be compared.

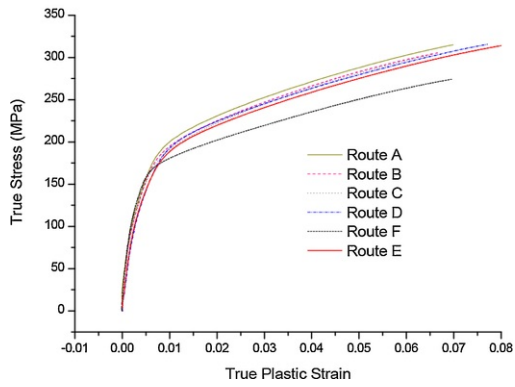
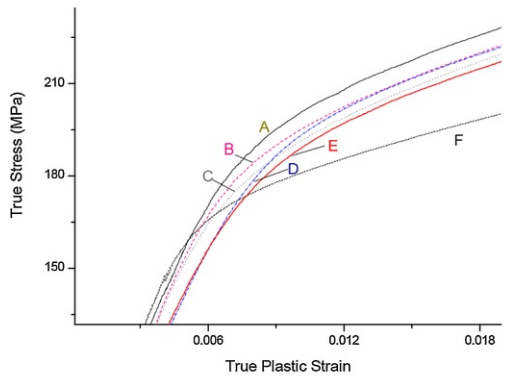
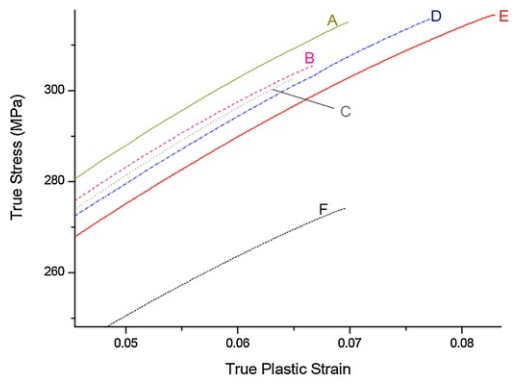


**Fig. 3** True stress-strain curves of the tensile tests.

alt-text: Fig. 3

**Table 2** Principal mechanical properties values (average values).

alt-text: Table 2

	Yield strength (MPa)	Tensile strength (MPa)	A (%)
Route A	173 ( $\sigma = 1.0$ )	285 ( $\sigma = 8.9$ )	6.4 ( $\sigma = 0.9$ )

Route B	169 ( $\sigma = 1.9$ )	278 ( $\sigma = 6.3$ )	6.1 ( $\sigma = 0.5$ )
Route C	164 ( $\sigma = 1.8$ )	278 ( $\sigma = 4.5$ )	6.4 ( $\sigma = 0.3$ )
Route D	157 ( $\sigma = 2.6$ )	287 ( $\sigma = 6.6$ )	7.6 ( $\sigma = 0.6$ )
Route E	156 ( $\sigma = 0.8$ )	288 ( $\sigma = 4.7$ )	8.1 ( $\sigma = 0.8$ )
Route F	162 ( $\sigma = 1.4$ )	175 ( $\sigma = 5.4$ )	6.9 ( $\sigma = 0.5$ )

Tensile strength values were similar except for Route F, which corresponds to the as-cast material. Differences appear in elongation values where routes D and E permit further deformation in the material prior to breakage. Plastic deformation occurs in all samples at very low loads, complicating any definition of the linear region. In the real stress-strain graph it can be compared the work hardening at low and high strains.

To study the strain hardening, a frequently used power law constitutive equation is considered:

$$\sigma = K\varepsilon^n \quad (1)$$

Where n is the strain hardening exponent obtained by power regression of 0.27 for all the routes. The work hardening rate is defined by:

$$\frac{d\sigma}{d\varepsilon} = kn\varepsilon^{(n-1)} = \frac{n\sigma}{\varepsilon} \quad (2)$$

The work hardening rate was obtained for various strain values and a plot has been constructed (Fig. 4). There are no differences at high strains but when the strain is low, the strain hardening rates of the DCT samples (Route D and E) are lower than that of the non-cryogenic treated samples.

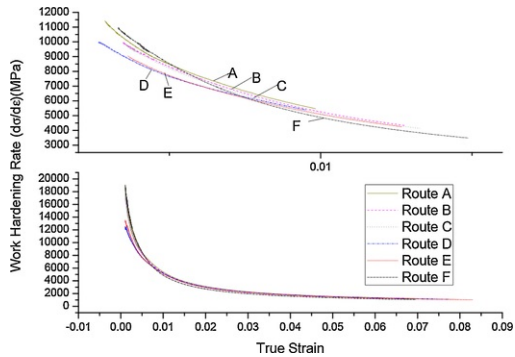


**Fig. 4** Strain hardening rate versus true strain of the treated samples.

alt-text: Fig. 4

The  $\beta$  precipitation phase of the supersaturated alloy after the solution treatment can take place continuously or discontinuously. Zhao et al. (2014) observed that discontinuous precipitation (DP) consists in the alternating growth of phase  $\beta$  plates along the grain boundaries and continuous precipitation (CP) within the grains forms much thinner acicular shapes. There was also established by Duly et al., (1995) that both types of precipitates coexist and compete for growth, although there are temperature ranges in which one type thrives more than another.

The microstructures of the samples following the two types of treatment T6 and T6 + DCT (Routes A and D), are shown in Fig. 5. In both cases, discontinuous precipitation was clearly observed.

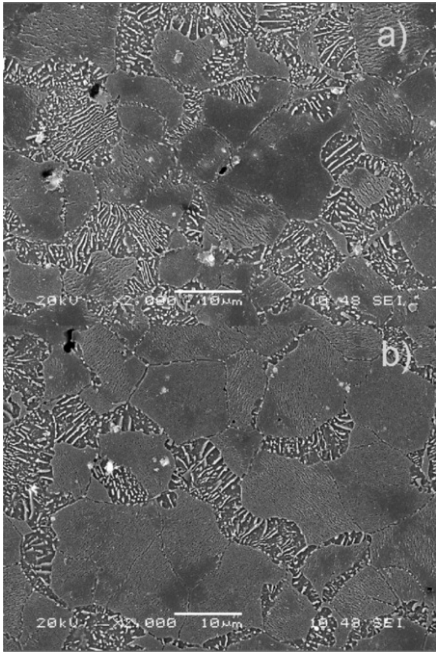


**Fig. 5** SEM of samples after heat treatment: (a) T6 (b) T6 + DCT.

alt-text: Fig. 5

A study of two solubilized and solubilized + DCT samples (Fig. 6) examined the differences provoked by cryogenic treatment in further detail. Grain size was measured by the intercept line method, resulting in  $13.5 \mu\text{m}$  ( $\sigma = 2.4$ ) in the center and  $11.2 \mu\text{m}$  ( $\sigma = 2.2$ ) at the edge, for the T6 sample, and,  $10.4 \mu\text{m}$  ( $\sigma = 1.6$ ) in the center and  $9.8 \mu\text{m}$  ( $\sigma = 1$ ) at the edge, for the T6 + DCT sample.

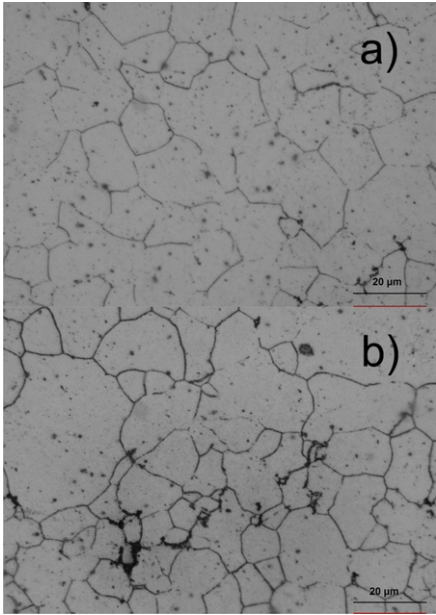


**Fig. 6** Samples (center zone) after a solution treatment: (a) T4 (b) T4 + DCT.

alt-text: Fig. 6

In the TEM study, two samples following routes A and D were compared. In the sample of Route A, numerous plate-shaped precipitates were found (Fig. 7a and b) which correspond to the discontinuous precipitates and also few areas with fine acicular-shaped precipitations that will be later discussed. In the Route D sample it was difficult to find the plate-shaped precipitation. However, numerous zones with fine acicular-shaped precipitates were observed (Fig. 7c and d). This last type of precipitates corresponds to the continuous precipitates. In Fig. 8, it can be observed the continuous precipitates at the same magnification for T6 and T6 + DCT samples.

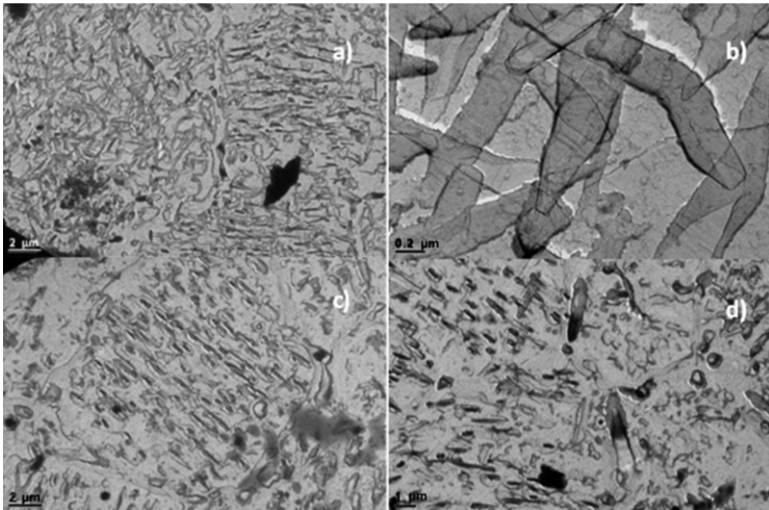


**Fig. 7** TEM images of samples. (a) Precipitation on a T6 sample; (b) plate-shaped precipitates on a T6 sample, (c) precipitation on a T6 + DCT sample; (d) lath-like precipitates on a T6 + DCT sample.

alt-text: Fig. 7

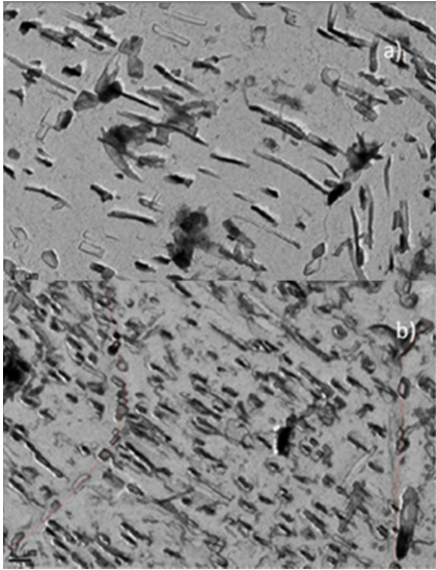


**Fig. 8** TEM images of continuous precipitates: (a) T6; (b) T6 + DCT.

alt-text: Fig. 8

## 4 Discussion

It has been observed that there is more continuous precipitation with cryogenic treatment. This is in agreement with the higher amount of precipitation observed also in ferrous alloys with a cryogenic treatment prior tempering. [Li et al. \(2013\)](#) studied DCT in as-cast samples and pointed out the fact that the difference in thermal expansion coefficient between  $\beta$  phase and magnesium matrix had an important influence in the appearance of dislocations. In this research the DCT is given after solution but there is still a difference in the concentration of aluminum from the edge to the center of each grain. [Liu et al. \(2012\)](#) observed a volume contraction and the decrease of lattice constant in the solid solution that provoked the precipitation of  $\beta$  phase. It could be concluded then, that cryogenic treatments cause some internal stresses due to shrinkage at low temperatures that causes defects such as dislocations and vacancies. [Braszczyńska-Malik \(2009\)](#) reported that the amount of continuous precipitation is dependent on the number of crystalline defects within the matrix, as they act as nucleation sites. At grain boundaries, the effect of precipitation is to form new edges and it therefore makes no contribution to the formation of more continuous precipitates.

Grain size decreased when cryogenic treatment was applied following solution. Although this point is relevant when analyzing the yield strength, as a reduction in grain size would increase the yield strength, it has no influence on the growth of discontinuous precipitates; [Duly and Brechet \(1994\)](#) reported that the DP rate of nucleation is not dependent on grain size at a solute content of between 5.4-10%.

The final fracture occurs when the numerous intergranular pores present in the alloys join and progress by the grain boundaries. The smaller the grain, the longer the path and then more energy is absorbed in the progression of the final breakdown. This allows higher elongation values and thus, higher tensile strengths when cryogenic treatment is applied.

The fact that T6 + DCT treatment decreases the yield strength might appear contradictory. Considering the factors that affect the yield strength for the AZ91 established by [Cáceres et al. \(2002\)](#), virtually all of them when applied to samples with cryogenic treatment would increase that value. These factors are precipitation-hardening, grain size and solid-solution hardening being this last one of less importance in AZ91 alloys. The contribution of work hardening is both positive and negative: positive, because the presence of atoms in solution can be expected to increase dislocation multiplication; and, negative because the formation of precipitation  $Mg_{17}Al_{12}$  provokes cross-slip and as a result dislocation tangles.

The principal mechanism is the first one, precipitation-hardening. According to [Celotto and Bastow, \(2001\)](#) and [Celotto \(2000\)](#), the hardening response of AZ91 at a given temperature is due to precipitation growth, especially because of the elongation of lath-shaped precipitates, rather than the nucleation of new precipitates. It is supposed that given an aging at a temperature, once most of the precipitates are nucleated,

the hardness begins to increase with the length and thickness of the precipitates. The TEM images and the theory suggest that there are a higher amount of precipitates with a cryogenic treatment. However, the yield strength decreases, so this could be due to the morphology of the precipitates.

If we observe the continuous precipitation that forms in a cryogenically treated sample (Fig. 8) and compare it with precipitation that forms on a sample with conventional treatment, it may be observed that although these are fewer in number in the second case, their shape is more elongated and a greater hardening effect may therefore be expected.

As seen in Fig. 4, at low strains there is difference between cryogenically treated and non-cryogenically treated samples, having the last ones a higher work hardening rate. A plausible reason could be that due to the cryogenic treatment, a higher amount of continuous precipitates form and this weakens the solution strengthening effect of Al in the Mg matrix. In addition, these precipitates have not the adequate length to be an effective barrier to the movement of the dislocations.

Then, it seems that the aging in the case of a cryogenic treatment prior aging should have been longer. Further work is taking place in this line because if the proportion of continuous precipitates could be increased and the size of them could be adequate, the age-hardening response would be improved substantially.

## 5 Conclusions

The introduction of a cryogenic treatment prior to aging in a T6 thermal treatment for AZ91D alloys has shown a beneficial effect, improvements in elongation while maintaining the same tensile strength. However, the yield strength has decreased, despite an increase in the amount of continuous precipitates, the longitudinal dimensions of which were not sufficient to maintain the yield strength. A slight decrease in grain size has also been observed.

The tensile strength depends on the elongation for HPDC AZ91 alloys. The porosity of the material is the reason of the final breakdown. The cracks propagate by the grain boundaries from the different pores. A decrease in the grain size improves the elongation increasing the path developing cracks. The cryogenic treatment decreases slightly the grain size and this is the main reason of the similar tensile strengths for T6 and T6 + DCT treatments.

These results are encouraging from a theoretical point of view and will lead to future studies on the way in which the dimensions of the precipitates may be affected and the relationships with variations in the variables of the cryogenic treatment and the aging treatments. The objective would be longer acicular precipitates that might increase the yield strength together with elongation.

## Acknowledgement

The authors wish to thank [Grupo Antolín Ingeniería S.A](#), for the financial support and the provision of samples for all tests.

## References

- Amini K., Akhbarizadeh A. and Javadpour S., Investigating the effect of quench environment and deep cryogenic treatment on the wear behavior of AZ91, *Mater. Des.* **54**, 2014, 154-160.
- Asl K.M., Tari A. and Khomamizadeh F., Effect of Deep cryogenic treatment on microstructure, creep and wear behaviors of AZ91 magnesium alloy, *Mater. Sci. Eng. A* **523**, 2009, 27-31.
- Braszczyńska-Malik K.N., Discontinuous and continuous precipitation in magnesium-aluminium type alloys, *J. Alloys Comp.* **477**, 2009, 870-876.
- Cáceres C.H., Davison C.J., Griffiths J.R. and Newton C.L., Effects of solidification rate and ageing on the microstructure and mechanical properties of AZ91 alloy, *Mater. Sci. Eng. A* **325**, 2002, 344-355.
- Cavaliere P. and De Marco P.P., Fatigue behaviour of friction stir processed AZ91 magnesium alloy produced by high pressure die casting, *Mater. Charact.* **58**, 2007, 226-332.
- Celotto S. and Bastow T.J., Study of precipitation in aged binary Mg-Al and ternary Mg-Al-Zn alloys using <sup>27</sup>Al NMR spectroscopy, *Acta Mater.* **49** (1), 2001, 41-51.
- Celotto S., TEM study of continuous precipitation in Mg-9%Wt%Al-1Wt%Zn alloy, *Acta Mater.* **48**, 2000, 1775-1787.
- Chen P., Malone T., Bond R. and Torres P., Effects of cryogenic treatment on the residual stress and mechanical properties of an aerospace aluminum alloy, *Proceedings of the 4th Conference on Aerospace Materials Processes and Environmental Technology* 2001.
- Duly D. and Brechet Y., Nucleation mechanism of discontinuous precipitation in Mg-Al alloys and relation with the morphology, *Acta Metall. Mater.* **42**, 1994, 3035-3043.

- Duly D., Simon J.P. and Brechet Y., On the competition between continuous and discontinuous precipitations in binary Mg-Al alloys, *Acta Metall. Mater.* **43** (1), 1995, 101-106.
- Ji S., Ma Q. and Fan Z., The creep behavior of rheo-diecast (Mg-9Al-1Zn) alloy, *Mater. Sci. Eng. A* **434**, 2006, 7-12.
- Jiang Y., Chen D., Chen Z. and Liu J., Effect of cryogenic treatment on the microstructure and mechanical properties of AZ31 magnesium alloy, *Mater. Manuf. Process.* **25**, 2010, 837-841.
- Jordine A., Increased life of carburized race car gears by cryogenic treatments, *Int. J. Fatigue* **18** (6), 1996, 418-424.
- Li G., Wang H., Cai Y., Zhao Y., Wang J. and Gill S.P.A., Microstructure and mechanical properties of AZ91 magnesium alloy subject to deep cryogenic treatments, *Int. J. Miner. Metall. Mater.* **20** (9), 2013, 896-901.
- Li X., Xiong S.M. and Guo Z., On the porosity induced by externally solidified crystals in high pressure die cast of AM60B alloy and its effect on crack initiation and propagation, *Mater. Sci. Eng. A* **633**, 2015, 35-41.
- Liu J., Li G., Chen D. and Chen Z., Effect of cryogenic treatment on deformation behavior of as-cast AZ91 Mg alloy, Chinese, *J. Aeronaut.* **25**, 2012, 931-936.
- Lulay K.E., Khan K. and Chaaya D., The effect of cryogenic treatments on 7075 aluminum alloys, *J. Mater. Eng. Perform.* **11** (5), 2002, 479-480.
- Luo A. and Pekguleryuz M.O., Review cast magnesium alloys for elevated temperature applications, *J. Mater. Sci.* **29**, 1994, 5259-5271.
- Mukai T., Yamanoi M., Watanabe H. and Higashi K., Ductility enhancement in AZ31 magnesium alloy by controlling its grain structure, *Scripta Mater.* **45**, 2001, 89-94.
- Preciado M., Bravo P.M. and Alegre J.M., Effect of low temperature tempering prior cryogenic treatment on carburized steels, *J. Mater. Proc. Tech.* **176**, 2006, 41-44.
- Wang L., Turnley P. and Savage G., Gas content in high pressure die castings, *J. Mater. Proc. Tech.* **211**, 2011, 1510-1515.
- Wetengen H., Magnesium alloys for structural application; recent advances, *J. Physique IV Colloque* **03** (C7), 1993, 491-501.
- Yuan C., Wang Y., Sang D., Li Y., Jing L., Fu R. and Zhang X., Effects of deep cryogenic treatment on the microstructure and mechanical properties of commercial pure zirconium, *J. Alloys Comp.* **619**, 2015, 513-519.
- Zhao D., Wang Z., Zuo M. and Geng H., Effects of heat treatment on microstructure and mechanical properties of extruded AZ80 magnesium alloy, *Mater. Des.* **56**, 2014, 589-593.

## Queries and Answers

**Query:** The author names have been tagged as given names and surnames (surnames are highlighted in teal color). Please confirm if they have been identified correctly

**Answer:** Name: Mónica Surname: Preciado Name: Pedro Miguel Surname: Bravo Name: David Surname: Cárdenas

**Query:** "Your article is registered as a regular item and is being processed for inclusion in a regular issue of the journal. If this is NOT correct and your article belongs to a Special Issue/Collection please contact h.lampard@elsevier.com immediately prior to returning your corrections."

**Answer:** Yes. It is a regular item.

**Query:** The citation "Duly et al., (1994)" in sentence "There was also established by" has been changed to "Duly et al., (1995)" to match the date in reference list, please check and correct if necessary.

**Answer:** It is OK

**Query:** One or more sponsor names and the sponsor country identifier may have been edited to a standard format that enables better searching and identification of your article. Please check and correct if necessary.

**Answer:** The sponsor country is Spain.

**Query:** Please check the layout of both the tables, and correct if necessary.

**Answer:** The layout of both tables are OK